

Negative Thermal Expansion and Magnetic Transition in Anti-Perovskite Structured $\text{Mn}_3\text{Zn}_{1-x}\text{Sn}_x\text{N}$ Compounds

Ying Sun,[‡] Cong Wang,^{‡,§} Yongchun Wen,[‡] Lihua Chu,[‡] Hui Pan,[§] and Man Nie[‡]

[‡]Department of Physics, Center for Condensed Matter and Materials Physics, Beihang University, Beijing 100191, China

[§]Laboratory of Micro-nano Measurement, Manipulation and Physics (Ministry of Education), Beihang University, Beijing 100083, China

Meibo Tang

Shanghai Institute of Ceramics, Chinese Academy of Sciences, Shanghai 200050, China

The thermal expansion properties of $\text{Mn}_3\text{Zn}_{1-x}\text{Sn}_x\text{N}$ ($x = 0.1, 0.2, 0.3, 0.5, 0.8, 1.0$) compounds were investigated by variable temperature X-ray powder diffraction. With increasing Sn content, the thermal expansion behavior of $\text{Mn}_3\text{Zn}_{1-x}\text{Sn}_x\text{N}$ changes from positive to negative and returns to positive near the magnetic transition temperature range. Moreover, the magnetic transition temperature increases from 185 to 495 K. It is interesting that the abnormal thermal expansion behavior of $\text{Mn}_3\text{Zn}_{1-x}\text{Sn}_x\text{N}$ is related to the number of valence electrons on Zn site and the equivalent effect with three valence electrons is beneficial for displaying negative thermal expansion. In addition, the antiferromagnetic order state gradually canted with the increasing Sn content due to the increase of Mn–Mn distance.

I. Introduction

ANTI-PEROVSKITE manganese compounds Mn_3XN ($\text{X} = \text{Ga}, \text{Al}, \text{Zn}, \text{Cu}, \text{and Sn}$) have attracted considerable attention during the last decade for their interesting physical properties,^{1–3} such as superconductivity,^{4,5} giant magnetoresistivity,⁶ and a nearly zero temperature coefficient of resistivity.⁷ However, little attention is paid for its thermal expansion properties. The discovery of large negative thermal expansion (NTE) effect in Ge-doped Mn_3CuN compounds has stimulated more research on the thermal expansion properties of $\text{Mn}_3\text{XN}(\text{C})$.^{8,9}

There always exists a magnetic phase transition in Mn_3XN with an increasing temperature, sometimes accompanied by a large lattice contraction. In our early work,¹⁰ we have reported that the lattice constant for Mn_3ZnN monotonically increases with temperature and never shows lattice contraction near the magnetic transition temperature. This phenomenon is quite different from the results in Kim *et al.*³ and Takenaka and Takagi⁸ in which an abrupt change of the lattice constant was observed near the magnetic transition temperature. However, partial substitution of Zn by Ge induces the lattice contraction behavior around the magnetic transition temperature. From the previous results, we concluded that the magnetic transition is necessary, but not enough for lattice contraction. Metal doping at X position also plays an important role for the lattice contraction, although the mechanism is not clear until now.

In Mn_3XN , the metal atoms on X sites offer itinerant electrons in the Fermi level. Hence, the valence electron number on Zn sites is a dominant factor for the structural, electronic, and magnetic transport properties of Mn_3ZnN . Only two valence electrons on the Zn site did not induce the NTE effect near the magnetic transition. However, the combination of Zn and Ge with three equivalent valence electrons produced the NTE effect. In Sun *et al.*,¹¹ we have reported that there existed a big abrupt drop of lattice constant for Mn_3GaN , which has three valence electrons on X site. Therefore, we speculate that Sn doping in Mn_3ZnN could also induce NTE phenomena as Sn and Ge have the same valence electrons. If so, it will provide an important evidence for the mechanism of NTE phenomenon. In addition, Takenaka *et al.*¹² have just reported the Sn-doping effect in Mn_3CuN and found that Sn doping did induce an NTE behavior from a normal thermal expansion, which strengthens our hypothesis.

In this paper, Sn-doping effects on the thermal expansion properties in Mn_3ZnN were investigated by variable temperature X-ray diffraction (XRD). The results indicated that the thermal expansion behavior varied from positive to negative, and returned to positive with the increasing Sn content. To further understand the origin of lattice contraction, the correlated magnetic transition was also analyzed.

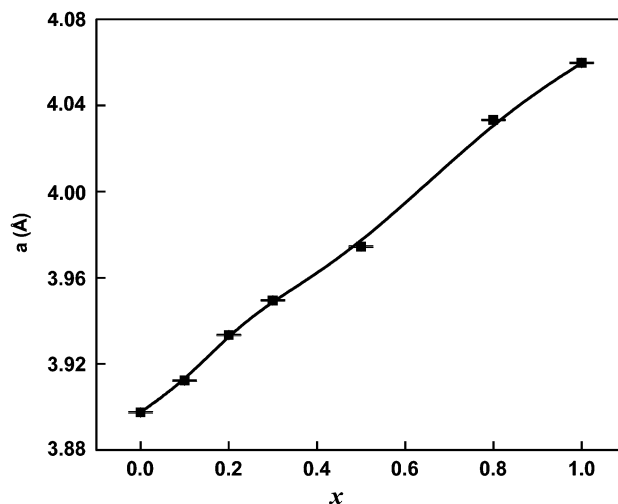


Fig. 1. Variation of lattice constant of $\text{Mn}_3\text{Zn}_{1-x}\text{Sn}_x\text{N}$ with x at room temperature.

R. L. Snyder—contributing editor

Manuscript No. 26965. Received October 20, 2009; approved February 2, 2010.

This work was financially supported by the National Natural Science Foundation of China (NSFC) (No. 50772008) and Key Laboratory of Micro-nano Measurement, Manipulation and Physics (Ministry of Education).

[†]Author to whom correspondence should be addressed. e-mail: congwang@buaa.edu.cn

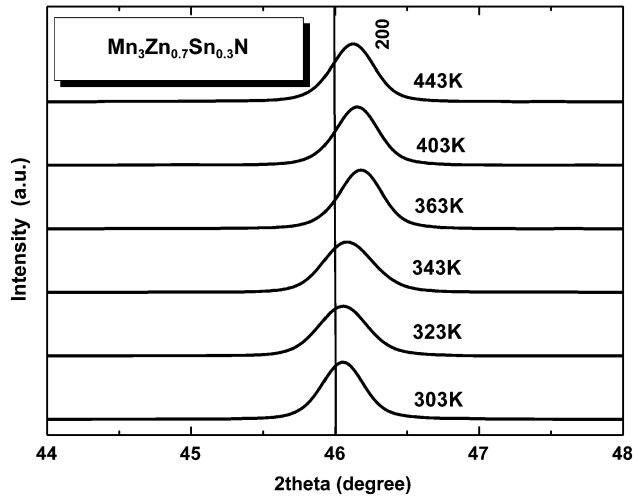


Fig. 2. Temperature dependence of the (200) XRD peak shifting for $\text{Mn}_3\text{Zn}_{0.7}\text{Sn}_{0.3}\text{N}$.

II. Experimental Procedure

Polycrystalline samples $\text{Mn}_3\text{Zn}_{1-x}\text{Sn}_x\text{N}$ were prepared by the solid-state reaction. The powders of Mn_2N , Zn, and Sn were intimately mixed in the desired ratio, then ground, and pressed into pellets. The pellets were wrapped in a Ta foil and sealed in a vacuumized quartz tube. Then, the quartz tube was sintered in a box furnace at 800°C for 60 h, and then cooled down to room temperature. The procedure was repeated until a single phase was successfully obtained.

XRD patterns of the samples were obtained using an X'Pert PRO powder diffractometer (PANalytical, Almelo, the Netherlands). Structural characterization showed that all of the samples were crystallized in the cubic lattice with the $Pm\bar{3}m$ space group. The crystallographic data of the specimens were calculated by Powder X software (Cheng Dong, Beijing, China).¹³ As shown in Fig. 1, the lattice constant increases with the increasing

Sn content. The result is well consistent with that the Zn atom is smaller than Sn and indirectly reveals that Sn atoms were successfully introduced into Zn positions.

Thermal expansion measurements were carried out using the variable temperature X'Pert PRO powder diffractometer. The samples were heated to the desired temperature at a rate of 10 K/min and held for 10 min. The XRD patterns at different temperatures were recorded, and then the lattice constants were calculated by indexing all of XRD peaks. $\chi(T)$ curves were measured with a SQUID magnetometer (Quantum Design Corporate, San Diego, CA) below room temperature and Lake Shore 7410 VSM (Lake Shore, Westerville, OH) above room temperature, respectively.

III. Results and Discussion

We measured the thermal expansion behaviors using variable temperature XRD. All of XRD patterns at different temperatures were compared carefully and only the shift of the peaks was found. In our samples, the lattice kept the cubic structure and no tetragonal distortion was observed over the entire measured temperature range. As shown in Fig. 2, the angle of the (200) peak for $\text{Mn}_3\text{Zn}_{0.7}\text{Sn}_{0.3}\text{N}$ first decreases with the increasing temperature, then increases abruptly from 343 to 363 K, which implies that a large isotropic lattice contraction occurred, and finally decreases with the further increasing temperature. Moreover, no peak splitting was observed, i.e. the cubic structure always remained. Temperature dependence of the lattice constant for $\text{Mn}_3\text{Zn}_{1-x}\text{Sn}_x\text{N}$ samples was shown in Fig. 3. When only a small amount of Sn was used to replace Zn, $\text{Mn}_3\text{Zn}_{0.9}\text{Sn}_{0.1}\text{N}$ still displayed a normal thermal expansion behavior accompanying with an antiferromagnetic (AFM) to paramagnetic (PM) transition near 220 K. The a - T curve is nearly linear and the linear thermal expansion coefficient is estimated to be $9.39 \times 10^{-6} \text{ K}^{-1}$ ($160 \text{ K} < T < 290 \text{ K}$). Surprisingly, when the Sn content increased to $x = 0.2$, there appeared a pronounced decrease in the lattice constant near 319 K, still together with an AFM-PM magnetic transition. The lattice constant reached a minimum at 352 K and then was followed by a

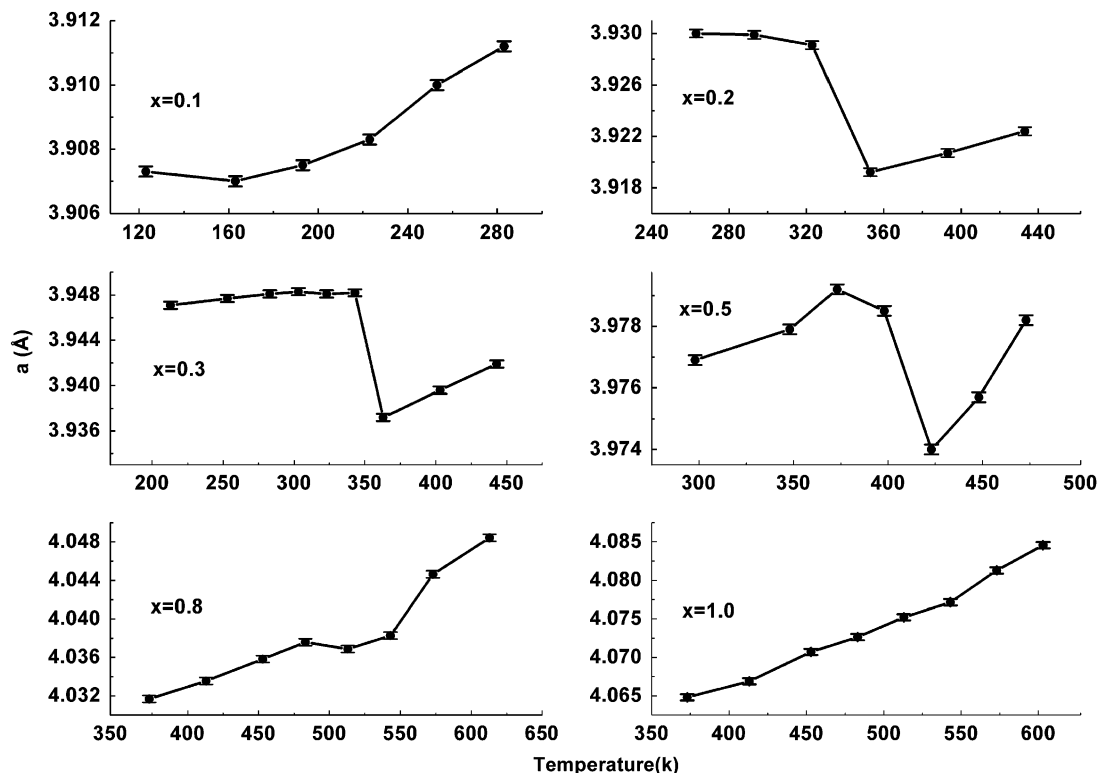


Fig. 3. Temperature dependence of the lattice constant for $\text{Mn}_3\text{Zn}_{1-x}\text{Sn}_x\text{N}$ by variable temperature XRD.

normal linear increase with further increasing temperature. When $x = 0.3$ and 0.5 for $\text{Mn}_3\text{Zn}_{1-x}\text{Sn}_x\text{N}$, the same results were obtained. However, when the Sn substitution increased to $x = 0.8$, the thermal expansion near the magnetic transition returned to normal, except for an anomaly from 480 to 530 K. For Mn_3SnN , the thermal expansion behavior became completely positive and the linear thermal expansion coefficient is $2.09 \times 10^{-5} \text{ K}^{-1}$. In summary, the Sn doping in $\text{Mn}_3\text{Zn}_{1-x}\text{Sn}_x\text{N}$ resulted in the thermal expansion behaviors changing from positive to negative and returning to positive. The NTE temperature ranges moved to a higher temperature with the increasing Sn content and was broadened to $\Delta T = 50 \text{ K}$ when $x = 0.5$.

What is the origin for displaying the lattice contraction during the magnetic transition temperature range? The magnetic transition does sometimes induce lattice contraction, but not always. This phenomenon reveals that the magnetic transition is not sufficient to introduce an obvious abrupt change of lattice constants. Thus, certainly there are other factors determining the abnormal thermal expansion behavior. In $\text{Mn}_3\text{Zn}_{1-x}\text{Sn}_x\text{N}$, the Mn atoms provide the localized magnetic moments responsible for the magnetism, while the metal atoms on Zn sites provide the itinerant electrons at the Fermi level. From the doping effects, the abnormal thermal expansion behaviors in $\text{Mn}_3\text{Zn}_{1-x}\text{Sn}_x\text{N}$ may be related to the different number of valence electrons on the Zn site. As we know, Zn has two free electrons with the arrangement: $3d^{10}4s^2$ and Sn have four free electrons with the arrangement: $5s^25p^2$. Only two or four valence electrons on the Zn site could not induce NTE. But their combination with three equivalent valence electrons has produced the NTE effect. Thus, it was very likely that the right electronic density of states triggered the lattice contraction in the magnetic transition temperature range. In Mn_3XN , the triply degenerated $p-d_{\text{II}}$ sub-band is near to the Fermi surface.¹⁴ Because of the different number of valence electrons, substitution of Zn by Sn changes the position of d_{II} and leads to a shift of the Fermi level. Jardin and Labbe¹⁵ have pointed out that the Fermi energy E_F lies very close to the infinite singularities energy E_S in the electronic density of states in Mn_3XN . As the Fermi energy E_F is smaller or larger than E_S , the structure transition is a first-order or second-order phase transition. When E_F just lies in E_S , the second-order transition is always obtained. With the increasing Sn content, the Fermi level shifts to the higher energy side. We suspect that the Fermi energy E_F for Mn_3ZnN and Mn_3SnN lies to two adjacent singularities, respectively, while the E_F for $\text{Mn}_3\text{Zn}_{1-x}\text{Sn}_x\text{N}$ ($0.0 < x < 1.0$) series compounds just lie between them. Thus, the abrupt drop of lattice constant near the magnetic transition occurred in $\text{Mn}_3\text{Zn}_{1-x}\text{Sn}_x\text{N}$ ($0.2 \leq x \leq 0.5$) whereas this did not exist in pure Mn_3ZnN and Mn_3SnN .

Similarly with Mn_3ZnN and Mn_3SnN , Mn_3CuN did not display lattice contraction in the magnetic transition region. When a certain amount of Sn was introduced into Mn_3CuN , there appeared a large lattice contraction near the magnetic transition temperature. However, Mn_3CuN doped with Zn did not exhibit lattice contraction. The same characterization for the compounds displaying the NTE effect is with three equivalent valence electrons at X site, such as $\text{Mn}_3\text{Zn}_{1-x}\text{Sn}_x\text{N}$, $\text{Mn}_3\text{Zn}_{1-x}\text{Ge}_x\text{N}$,¹⁰ $\text{Mn}_3\text{Cu}_{1-x}\text{Sn}_x\text{N}$, and Mn_3GaN .¹¹ All of the results are in agreement with the above analysis and indirectly verifies the above conclusion about the abnormal variation of the thermal expansion behaviors in $\text{Mn}_3\text{Zn}_{1-x}\text{Sn}_x\text{N}$. Further studies are being carried out to further clarify the mechanism of the abnormal thermal expansion in $\text{Mn}_3\text{Zn}_{1-x}\text{Sn}_x\text{N}$.

As clearly seen in Fig. 4, the $\chi(T)$ curve showed an AFM-PM transition with the increasing temperature in the $\text{Mn}_3\text{Zn}_{1-x}\text{Sn}_x\text{N}$ compound when $x \leq 0.5$. We noticed that the doping of Sn element in Mn_3ZnN not only drove the transition temperature to a higher temperature but also weakened the AFM-PM transition peak. Further increasing the Sn content, the AFM-PM transition collapses when $x = 0.8$ and 1.0 . In order to testify this, the $\chi(T)$ curve for $x = 1.0$ below room temperature was obtained and no AFM-PM transition peak was detected, as shown in the inset of Fig. 4. Thus, we think that the

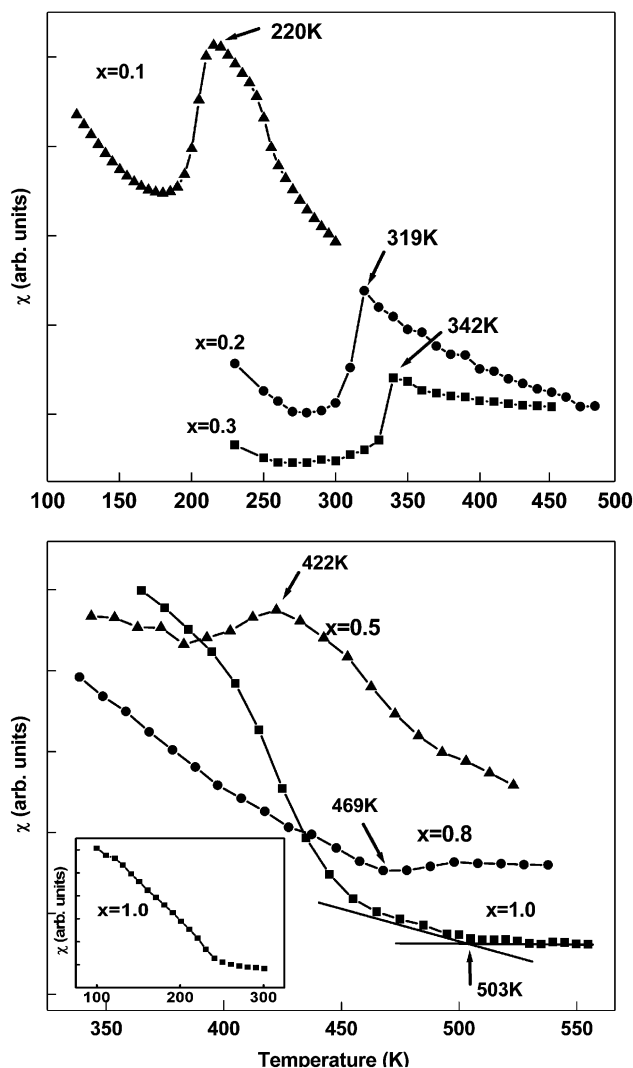


Fig. 4. Temperature dependence of the magnetic susceptibility for $\text{Mn}_3\text{Zn}_{1-x}\text{Sn}_x\text{N}$.

transition from canted antiferromagnetic (CAF) to paramagnetic occurred for $x = 0.8$ and 1.0 at 465 and 495 K, respectively, i.e. the antiferromagnetic spin state turns to canted spin order with increasing Sn content. The canted antiferromagnetic behavior mainly comes from the decreasing of antiferromagnetic exchange interaction as the Mn-Mn distance increases with the Sn content.

With the increasing Sn-doping content, the magnetic transition temperature shifts from 185 K for $x = 0$ to 495 K for $x = 1.0$. Fruchart and Bertaut¹⁴ has referred that $\zeta = Kn_v(r_{a0} + \Delta r_a)/r_a$. In the equation, the phenomenological quantity ζ has the dimension of an electron concentration. n_v is the number of valence electrons of X atom, r_a is atomic radius of X, Δr_a the difference of radius between X the element and X in the perovskite structure, and K is a normalizing constant. The transition temperature is proportional to ζ , and thus the “electron concentration” around the metal X is a key factor for the variation of the magnetic transition temperature. From the equation, we can conclude that the large difference of the magnetic transition temperature in $\text{Mn}_3\text{Zn}_{1-x}\text{Sn}_x\text{N}$ mainly comes from their different valence electrons of Zn and Sn elements.

IV. Conclusion

$\text{Mn}_3\text{Zn}_{1-x}\text{Sn}_x\text{N}$ ($x = 0, 0.1, 0.2, 0.3, 0.5, 0.8$, and 1.0) samples were prepared by the solid-state reaction and their thermal ex-

pansion properties were studied using variable temperature XRD. The indexing results indicated that replacing Zn atoms by larger Sn atoms led to an increase of the lattice constant, whereas the crystal structure was still cubic lattice with $Pm\bar{3}m$ space group. With the increasing Sn concentration, the thermal expansion behaviors varied from positive to negative, and returned to positive at the temperature range near the magnetic transition. Although pure Mn_3ZnN and Mn_3SnN did not show any lattice contraction at the magnetic transition temperature, their solid solution displayed a very interesting thermal expansion phenomenon. It is possible that the variation of valence electrons on Zn sites changed the electronic density of states at the Fermi level, and thus led to the abnormal change of the lattice constant for $Mn_3Zn_{1-x}Sn_xN$. From the experimental results, we think that only two or four valence electrons on the Zn site cannot produce NTE, but the equivalent effect with three valence electrons is advantageous for NTE, besides the factor in the change of spin states. Thus, the control of the variation of lattice constant in Mn_3XN can be achieved by adjusting the number of the valence electrons on X sites because the electronic density of states at the Fermi level is a key factor for the thermal expansion behaviors in this kind of materials.

References

- ¹E. F. Bertaut, D. Fruchart, J. P. Bouchaud, and R. Fruchart, "Neutron Diffraction of Mn_3GaN ," *Solid State Commun.*, **6** [5] 251–6 (1968).
- ²T. He, Q. Huang, A. P. Ramirez, Y. Wang, K. A. Regan, N. Rogado, M. A. Hayward, M. K. Haas, J. S. Slusky, K. Inumara, H. W. Zandbergen, N. P. Ong, and R. J. Cava, "Superconductivity in the Non-Oxide Perovskite $MgCNi_3$," *Nature*, **411**, 54–6 (2001).
- ³W. S. Kim, E. O. Chi, J. C. Kim, N. H. Hur, K. W. Lee, and Y. N. Choi, "Cracks Induced by Magnetic Ordering in the Antiperovskite $ZnNMn_3$," *Phys. Rev. B*, **68**, 172402, 4pp (2003).
- ⁴H. Rosner, R. Weht, M. D. Johannes, W. E. Pickett, and E. Tosatti, "Superconductivity near Ferromagnetism in $MgCNi_3$," *Phys. Rev. Lett.*, **88**, 027001, 4pp (2002).
- ⁵A. F. Dong, G. C. Che, W. W. Huang, S. L. Jia, H. Chen, and Z. X. Zhao, "Synthesis and Physical Properties of $AlCNi_3$," *Physica C*, **422**, 65–9 (2005).
- ⁶K. Kamishima, T. Goto, H. Nakagawa, N. Miura, M. Ohashi, N. Mori, T. Sasaki, and T. Kanomata, "Giant Magnetoresistance in the Intermetallic Compound Mn_3GaC ," *Phys. Rev. B*, **63**, 024426, 6pp (2000).
- ⁷E. O. Chi, W. S. Kim, and N. H. Hur, "Nearly Zero Temperature Coefficient of Resistivity in Antiperovskite Compound $CuNMn_3$," *Solid State Commun.*, **120**, 307–10 (2001).
- ⁸K. Takenaka and H. Takagi, "Giant Negative Thermal Expansion in Ge-Doped Anti-Perovskite Manganese Nitrides," *Appl. Phys. Lett.*, **87**, 261902, 3pp (2005).
- ⁹K. Takenaka and H. Takagi, "Magnetovolume Effect and Negative Thermal Expansion in $Mn_3(Cu_{1-x}Ge_x)N$," *Mater. Trans.*, **47** [3] 471–4 (2006).
- ¹⁰Y. Sun, C. Wang, Y. C. Wen, K. G. Zhu, and J. T. Zhao, "Lattice Contraction and Magnetic and Electronic Transport Properties of $Mn_3Zn_{1-x}Ge_xN$," *Appl. Phys. Lett.*, **91**, 231913, 3pp (2007).
- ¹¹Y. Sun, C. Wang, and Y. C. Wen, "Negative Thermal Expansion in $Mn_3Ga(Ge,Si)N$ Anti-Perovskite Materials," *Mater. Sci. Forum*, **561–565**, 557–62 (2007).
- ¹²K. Takenaka, K. Asano, M. Misawa, and H. Takagi, "Negative Thermal Expansion in Ge-Free Antiperovskite Manganese Nitrides: Tin-Doping Effect," *Appl. Phys. Lett.*, **92**, 011927, 3pp (2008).
- ¹³C. Dong, "PowderX: Windows-95-Based Program for Powder X-Ray Diffraction Data Processing," *J. Appl. Cryst.*, **32**, 838–9 (1999).
- ¹⁴D. Fruchart and E. F. Bertaut, "Magnetic Studies of the Metallic Perovskite-Type Compounds of Manganese," *J. Phys. Soc. Jpn.*, **44** [3] 781–91 (1978).
- ¹⁵J. P. Jardin and J. Labbe, "Phase Transitions and Band Structure in Metallic Perovskites (Carbides and Nitrides)," *J. Solid State Chem.*, **46**, 275–93 (1983). □